Am J Physiol Gastrointest Liver Physiol 316: G527–G538, 2019.
First published February 21, 2019; doi:10.1152/ajpgi.00148.2018.

RESEARCH ARTICLE | *Liver and Biliary Tract Physiology/Pathophysiology*

Inhibition of soluble epoxide hydrolase ameliorates hyperhomocysteinemia-induced hepatic steatosis by enhancing β-oxidation of fatty acid in mice

Liu Yao,[1] Boyang Cao,[1] Qian Cheng,[1] Wenbin Cai,[1] Chenji Ye,[1] Jing Liang,[1] Wenli Liu,[1] Lu Tan,[2] Meng Yan,[1] Bochuan Li,[1] Jinlong He,[1] Sung Hee Hwang,[3] Xu Zhang,[1] Chunjiong Wang,[1] Ding Ai,[1] Bruce D. Hammock,[3] and Yi Zhu[1]

[1]*Tianjin Key Laboratory of Metabolic Diseases; Key Laboratory of Immune Microenvironment and Disease (Ministry of Education); Collaborative Innovation Center of Tianjin for Medical Epigenetics and Department of Physiology and Pathophysiology, Tianjin Medical University, Tianjin, China;* [2]*Department of Laboratory Animal Science and Technology, Tianjin Medical University, Tianjin, China; and* [3]*Department of Entomology and Nematology and University of California, Davis Comprehensive Cancer Center, Davis, California*

Submitted 3 May 2018; accepted in final form 15 January 2019

Yao L, Cao B, Cheng Q, Cai W, Ye C, Liang J, Liu W, Tan L, Yan M, Li B, He J, Hwang SH, Zhang X, Wang C, Ai D, Hammock BD, Zhu Y. Inhibition of soluble epoxide hydrolase ameliorates hyperhomocysteinemia-induced hepatic steatosis by enhancing β-oxidation of fatty acid in mice. *Am J Physiol Gastrointest Liver Physiol* 316: G527–G538, 2019. First published February 21, 2019; doi:10.1152/ajpgi.00148.2018.—Hepatic steatosis is the beginning phase of nonalcoholic fatty liver disease, and hyperhomocysteinemia (HHcy) is a significant risk factor. Soluble epoxide hydrolase (sEH) hydrolyzes epoxyeicosatrienoic acids (EETs) and other epoxy fatty acids, attenuating their cardiovascular protective effects. However, the involvement of sEH in HHcy-induced hepatic steatosis is unknown. The current study aimed to explore the role of sEH in HHcy-induced lipid disorder. We fed 6-wk-old male mice a chow diet or 2% (wt/wt) high-metnionine diet for 8 wk to establish the HHcy model. A high level of homocysteine induced lipid accumulation in vivo and in vitro, which was concomitant with the increased activity and expression of sEH. Treatment with a highly selective specific sEH inhibitor (0.8 $mg \cdot kg^{-1} \cdot day^{-1}$ for the animal model and 1 μM for cells) prevented HHcy-induced lipid accumulation in vivo and in vitro. Inhibition of sEH activated the peroxisome proliferator-activated receptor-α (PPAR-α), as evidenced by elevated β-oxidation of fatty acids and the expression of PPAR-α target genes in HHcy-induced hepatic steatosis. In primary cultured hepatocytes, the effect of sEH inhibition on PPAR-α activation was further confirmed by a marked increase in PPAR-response element luciferase activity, which was reversed by knock down of PPAR-α. Of note, 11,12-EET ligand dependently activated PPAR-α. Thus increased sEH activity is a key determinant in the pathogenesis of HHcy-induced hepatic steatosis, and sEH inhibition could be an effective treatment for HHcy-induced hepatic steatosis.

NEW & NOTEWORTHY In the current study, we demonstrated that upregulation of soluble epoxide hydrolase (sEH) is involved in the hyperhomocysteinemia (HHcy)-caused hepatic steatosis in an HHcy mouse model and in murine primary hepatocytes. Improving hepatic steatosis in HHcy mice by pharmacological inhibition of sEH to activate peroxisome proliferator-activated receptor-α was ligand dependent, and sEH could be a potential therapeutic target for the treatment of nonalcoholic fatty liver disease.

Address for reprint requests and other correspondence: Y. Zhu, Dept. of Physiology and Pathophysiology, Tianjin Medical Univ., Tianjin, 300070, China (e-mail: zhuyi@tmu.edu.cn).

β-oxidation; hepatocytes; hyperhomocysteinemia; proliferator-activated receptor-α; soluble epoxide hydrolase

INTRODUCTION

Nonalcoholic fatty liver disease (NAFLD), characterized by excess lipid accumulation in liver, is one of the most common forms of chronic liver disease, ranging from simple steatosis to steatohepatitis, advanced fibrosis, and cirrhosis (2). The overall prevalence of NAFLD was reported to be 25.2%, with the highest prevalence reported from South America (30.5%) and the Middle East (31.8%) (57).

Methionine is an essential amino acid enriched in eggs, chicken breast, fish, dairy products, and many vegetables. Homocysteine is a toxic nonprotein sulfur containing amino acid after removal of the methyl group from methionine on *S*-adenosylmethionine (23). Individuals who consume a large amount of animal protein may ingest 2–3 g of methionine, which results in postprandial Hcy concentrations >20 μmol/l (50). Genetic abnormalities, age, sex and various nutritional and hormonal determinants contribute to hyperhomocysteinemia (HHcy). HHcy, defined by elevated plasma Hcy level (>15 μM), is an important and independent factor involved in several disorders, including atherosclerosis, diabetes, and immune activation (3, 8, 45). Epidemical study indicated a high prevalence of HHcy and NAFLD in Chinese adults, 18% with plasma Hcy concentrations ≥16.0 μM (16) and over a quarter affected by NAFLD (12, 28, 53). Moreover, elevated homocysteine levels were reported in patients with NAFLD (15). Clinical studies also demonstrated elevated homocysteine level positively associated with the prevalence of NAFLD (9, 10). Accumulating evidence revealed that HHcy disturbs lipid metabolism in the liver. Cystathionine β-synthase deficiency causes severe HHcy and leads to hepatic steatosis in mice (43, 52). We recently reported that HHcy induced by a high-methionine diet (HMD) led to hepatic steatosis by activating the aryl hydrocarbon receptor-CD36 pathway (56). However, a treatment for HHcy-induced hepatic steatosis is still lacking.

Soluble epoxide hydrolase (sEH) is a cytosolic enzyme with epoxide hydrolase and lipid phosphatase activities that cata-

Table 1. *Composition of the experimental diets*

Ingredient	Chow Diet, g/kg	HMD
Casein	200	200
Cornstarch	397.5	382.7
Dextrinized cornstarch	132	132
Sucrose	100	100
Cellulose	50	50
Soybean oil	70	70
Mineral mixture	35	35
Vitamin mixture	10	10
L-cystine	3	3
L-methionine		14.8
Choline bitartrate	2.5	2.5

HMD, 2% high methionine diet. Chow diet and HMD are based on AIN-93G rodent diets. Note: casein contains 5.2 L-methionine.

lyzes the rapid hydrolysis of all four epoxyeicosatrienoic acid (EET) regioisomers (5,6-; 8,9-; 11,12-; and 14,15-EET) to an inactive or less active diol, respectively, in addition to many other expoxy fatty acids (EpFAs) (33). We previously demonstrated that HHcy transcriptionally upregulated sEH, which resulted in endothelial injury that may contribute to the development of atherosclerosis (59). Inhibition of sEH ameliorated chronic high-fat diet-induced hepatic steatosis by reducing the systemic inflammatory status in mice (31). As the metabolites of the cytochrome-*P*450 oxidase pathway from arachidonic acid, EETs have potent anti-inflammatory and cardiovascular protective effects. Recently, EETs were found to participate in regulating lipid metabolism (58). EETs protected HepG2 cells against palmitic acid-induced inflammation and oxidative stress in vitro (7). Collectively, these findings suggest that increased sEH activity may contribute to HHcy-induced hepatic lipid disorder.

Hepatic steatosis represents excess accumulation of triglycerides in hepatocytes. Perturbations affecting lipid availability and disposal contribute to hepatic lipid disturbance (40). Fatty acid β-oxidation regulated by peroxisome proliferator-activated receptor-α (PPAR-α) is a critical event of consumption of lipids in the liver (4, 5). PPAR-α regulates lipid homeostasis by activating the transcription of a family of genes containing a PPAR-response element (PPRE). In essence, PPAR-α is a lipid sensor, and ineffective PPAR-α sensing can lead to reduced energy expenditure, thereby leading to hepatic steatosis (17). Importantly, EETs were verified as potent activators of PPAR-α in primary rat hepatocytes (35). However, their role in HHcy-induced hepatic steatosis is unknown.

Table 3. *Related variable index in mice fed a chow diet or high-methionine diet at 8 wk*

Variable Index	Chow Diet	HMD
Body weight, g	25.57 ± 0.73	25.70 ± 0.39
Liver/body weight ratio	0.042 ± 0.000	0.047 ± 0.001**
Plasma Hcy, μM	3.34 ± 0.80	20.58 ± 2.18**
Plasma TG, mM	0.51 ± 0.41	0.52 ± 0.04
Plasma Chol, mM	1.67 ± 0.10	1.92 ± 0.08

Data are means ± SE. HMD, high-metnionine diet; Hcy, homocysteine; TG, triglyceride; Chol, cholesterol. $^{**}P < 0.01$ vs. chow diet ($n = 6$ for chow diet; $n = 8$ for HMD).

The aim of our study was to investigate the potential benefits of sEH inhibition in HHcy-induced hepatic steatosis. Then, by using an HHcy mouse model, we studied the effect of sEH on hepatic lipid disturbance. Our findings indicated that upregulation of sEH is involved in HHcy-caused hepatic steatosis in vivo and in vitro. Inhibition of sEH attenuates fatty liver by activating PPAR-α. Thus elevated levels of EETs are beneficial for HHcy-induced hepatic steatosis, and sEH could be a potential therapeutic target for treating NAFLD.

MATERIALS AND METHODS

Reagents. L-methionine and DL-homocysteine were from Sigma-Aldrich (St. Louis, MO). RNA extraction kits were from BioTeke

Table 2. *Mouse primer sequences*

Gene	Sense	Antisense
sEH	5′-GGACGACGGAGACAAGAGAG-3′	5′-CTGTGTTGTGGACCAGGATG-3′
Lxrα	5′-TGCCATCAGCATCTTCTCTG-3′	5′-GGCTCACCAGCTTCATTAGC-3′
Srebp1	5′-ACTTCTGGAGACATCGCAAAC-3′	5′-GGTAGACAACAGCCGCATC-3′
Fasn	5′-TGGGTTCTAGCCAGCAGAGT-3′	5′- ACCACCAGAGACCGTTATGC-3′
Acc	5′-TGGTCGTGACTGCTCTGTGC-3′	5′-GTAGCC GAGGGTTCAGTTCC-3′
Chrebp	5′-TTACTGGAAGCGGCGCATCG-3′	5′-CCAAGCAGCACAGGCACCAC-3′
PPAR-α	5′-GTGGGTGGTTGAATCGTGAG-3′	5′-GCAGTGGAGTTTGGGTTGG-3′
Cpt1α	5′-ACGTTGGACGAATCGGAACA-3′	5′-GGTGGCCATGACATACTCCC-3′
Acox1	5′-CCGTCGAGAAATCGAGAACT-3′	5′-ATTGAGGCCAACAGGTTCCA-3′
Scad	5′-ATGTGCCAGAGGAGCTGAGT-3′	5′-TGATCCACTGTTGCTTCTGC-3′
Mcad	5′-AACTAAACATGGGCCAGCGA-3′	5′-CAGCTGCGACTGTAGGTCTG-3′
Lcad	5′-GCATCAACATCGCAGAGAAA-3′	5′-ACGCTTGCTCTTCCCAAGTA-3′
apoB	5′-TCACCATTTGCCCTCAACCTAA-3′	5′-GAAGGCTCTTTGGAAGTGTAAAC-3′
Mtp	5′-ATCATCATTGGAGCCCTGGT-3′	5′-CATTCTTCAGGGCCAGCA-3′
PPAR-γ	5′-ACCACTCGCATTCCTTT-3′	5′-CACAGACTCGGGCACTCA-3′
CD36	5′-TGGTCAAGCCAGCTAGAAA-3′	5′-CCCAGTCTCATTTAGCCAC-3′
Fatp1	5′-CCGTATCCTCACGCATGTGT-3′	5′-CTCCATCGTGTCCTCATTGAC-3′
Fatp2	5′-GATGCCGTGTCCGTCTTTTAC-3′	5′-GACTTCAGACCTCCACGACTC-3′
Fatp5	5′-TCGGATCTGGGAATTCTACG-3′	5′-TTGGTTCTTTCGAACCTTGG-3′
Fabp1	5′-GCCAGGAGAACTTTGAGC-3′	5′-TTGACGACTGCCTTGACT-3′
β-Actin	5′-CTGTCCCTGTATGCCTCT-3′	5′-ATGTCACGCACGATTTCC-3′

sEH, soluble epoxide hydrolase; PPAR-α, peroxisome proliferator-activated receptor-α; Cpt1a, carnitine palmitoyl transferase 1a; Acox1, acyl-coenzyme A oxidase 1; Scad, Mcad, and Lcad, short-, medium- and long-chain acyl-coenzyme A dehydrogenase; Fatp, fatty acid transporter protein; Fabp, fatty acid binding protein.

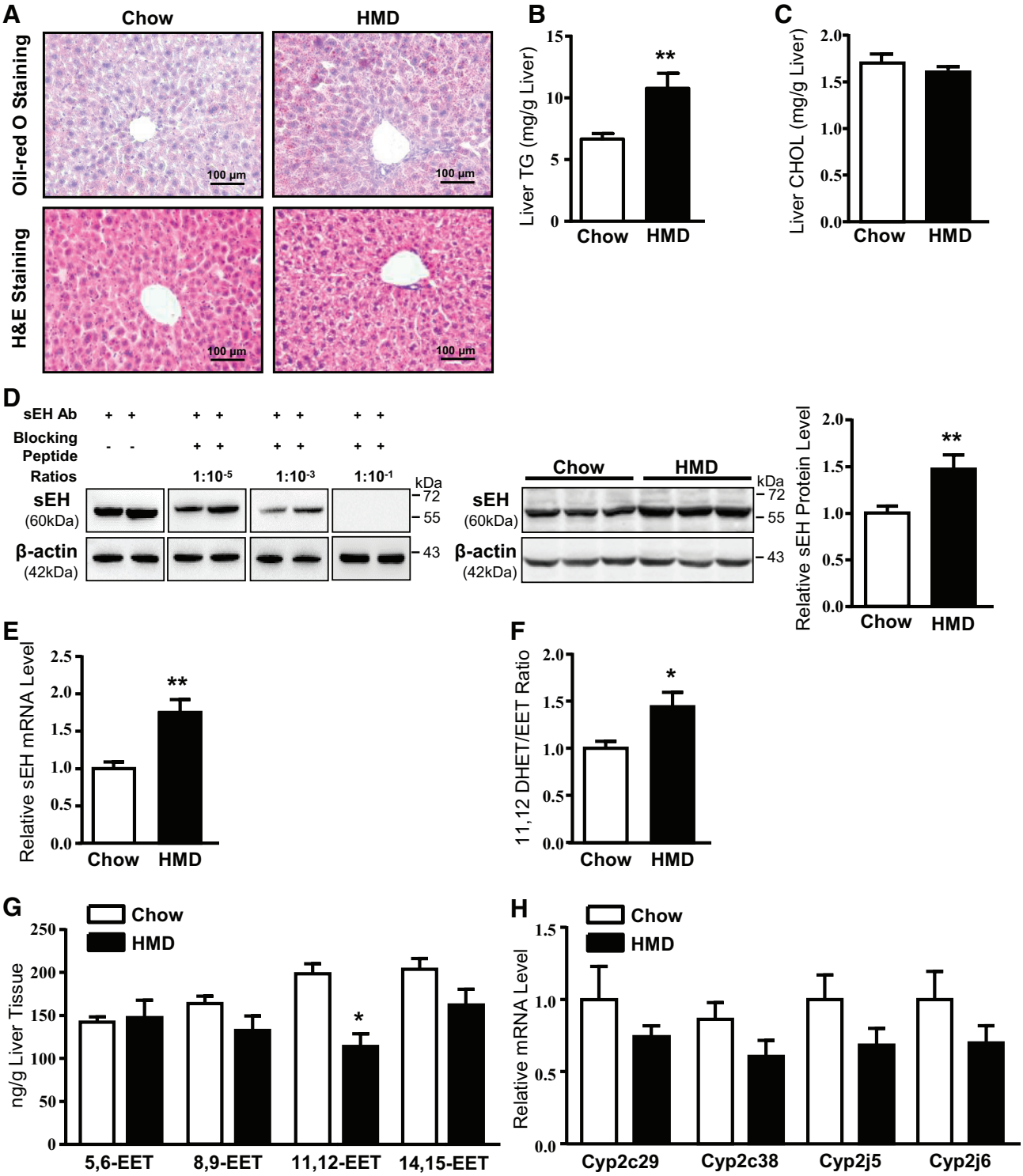

Fig. 1. Effect of hyperhomocysteinemia (HHcy) on lipid accumulation and soluble epoxide hydrolase (sEH) expression and activity in vivo. Male C57BL/6 mice (6 wk old) were fed a standard chow diet or 2% (wt/wt) L-methionine diet for 8 wk. *A*: Oil-red O staining (*top*) and hematoxylin and eosin (H&E) staining (*bottom*) of livers in representative sections. Images were taken at ×200 magnification. *B* and *C*: hepatic triglyceride and cholesterol content. *D*: Western blot analysis of the specificity of sEH antibody by sEH blocking peptide in the control mice liver tissue (*left*). Ab, antibody. The ratios represented sEH antibody to blocking peptide. Western blot analysis and quantification of sEH protein content (*right*) in the liver of mice fed a high-methionine diet (HMD). β-Actin was an internal control. *E*: quantitative (q)PCR analysis of the mRNA level of sEH. *F*: sEH activity was evaluated by the metabolic rate of 11,12-dihydroxyeicosatrienoic acid (DHET) to 11,12-epoxyeicosatrienoic acid (EET) by liquid chromatography with tandem mass spectrometry (LC-MS/MS). *G*: LC-MS/MS analysis of each regioisomer of EET level in the liver (*right*). *H*: qPCR analysis of mRNA levels of genes involved in EETs synthesis. Data are means ± SE by unpaired *t*-test; $n = 6$ for chow diet; $n = 8$ for HMD. $^{*}P < 0.05$; $^{**}P < 0.01$ vs. Chow.

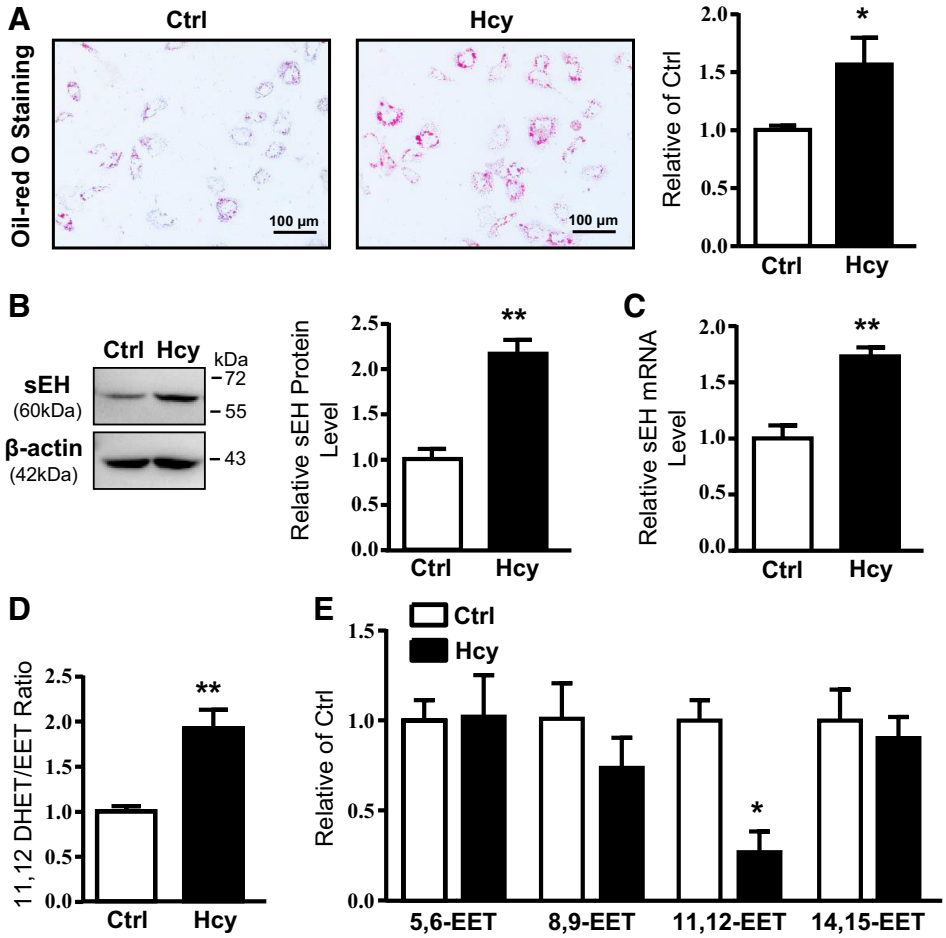

Fig. 2. Effect of hyperhomocysteinemia (HHcy) on lipid accumulation and the expression of soluble epoxide hydrolase (sEH) in primary hepatocytes. Murine primary hepatocytes were cultured and treated with Hcy (100 μM) for 24 h. *A*: Oil-red O staining of representative images (*left*) and quantification (*right*) of intracellular lipid deposition. Images were taken at ×200 magnification. *B*: Western blot analysis (*top*) and quantification (*bottom*) of sEH protein level. β-Actin was an internal control. *C*: mRNA level of sEH in Hcy-treated hepatocytes. *D*: sEH activity was evaluated by the metabolic rate of 11,12-dihydroxyeicosatrienoic acid (DHET) to 11,12-epoxyeicosatrienoic acid (EET) by liquid chromatography with tandem mass spectrometry (LC-MS/MS). *E*: LC-MS/MS analysis of each regioisomer of EET level in hepatocytes. Data are means ± SE of 3 independent experiments by unpaired *t*-test. $*P < 0.05$; $**P < 0.01$ vs. Ctrl.

(Beijing). Quantitative real-time PCR (qPCR) involved the use of PTC-200 with reagents from Stratagene (Zhejiang, China). Antibodies against sEH and PPAR-α were from Cayman Chemical (Ann Arbor, MI); sEH blocking peptide was from Cayman Chemical; antibodies against carnitine palmitoyl transferase 1a (Cpt1a), acyl-coenzyme A oxidase 1 (Acox1), medium chain acyl-coenzyme A dehydrogenase (Mcad), and β-actin were from Proteintech (Chicago, IL). An anti-rabbit or anti-mouse (Cell Signaling Technology, Boston, MA) IgG horseradish peroxidase-conjugated secondary antibody was from Cell Signaling Technology (Boston, MA). The luciferase reporter assay system was from Promega (Madison, WI), and the transfection reagent Lipofectamine3000 was from Invitrogen (Carlsbad, CA). Small interfering RNA (siRNA) targeting PPAR-α was from Santa Cruz Biotechnology (Santa Cruz, CA).

Animals and treatments. The specific-pathogen-free C57BL/6 mice from the Experimental Animal Centre of Military Medical Science Academy (Beijing) were fed a standard laboratory chow diet under a 12-h:12-h light-dark cycle. Six-week-old male mice received the control chow diet or a metnionine-enriched diet (Table 1) for 8 wk. To study the effect of selective sEH inhibitor 1-trifluoromethoxyphenyl-3-(1-propionylpiperidin-4-*yl*) urea (TPPU) on HHcy-induced metabolic disorders, mice were divided into three groups: mice were fed the control diet or metnionine-enriched diet for 4 wk, and then half of the metnionine-enriched diet fed mice were given TPPU (0.8 $mg \cdot kg^{-1} \cdot day^{-1}$ added in 1% final volume polyethylene glycol 400 for sEH inhibition) from the fifth week. When the experiment ended, all animals were deeply anesthetized with isoflurane and perfused transcardially with 10 ml isotonic saline. Blood serum was isolated after centrifugation for measuring total Hcy level by the enzymatic recycling assay. Livers were removed and postfixed for immunohistochemistry. The investigation conformed to the *Guide for the Care and Use of Laboratory Animals* by the National Institutes of Health (NIH Publication No. 85-23, updated 2011). Study protocols and use of animals were approved by Institutional Animal Care and Use Committee of Tianjin Medical University, Tianjin, China.

Culture of murine primary hepatocytes. Murine primary hepatocytes were isolated as described previously (51). Five- to 6-wk-old male C57BL/6 mice were anaesthetized with isoflurane. The free inferior vena cava was perfused with heparin, solution I (Krebs solution + 0.1 mM EGTA), and solution II (Krebs solution + 2.74

Table 4. *Related variables in chow- and HMD fed and HMD + soluble epoxide hydrolase inhibitor (TPPU) mice*

Variable Index	Chow Diet	HMD	HMD+TPPU
Body weight, g	25.09 ± 0.84	25.44 ± 0.43	25.39 ± 0.66
Liver/body Weight ratio	0.038 ± 0.000	0.046 ± 0.000**	0.043 ± 0.000#
Plasma Hcy, μM	3.13 ± 0.87	27.79 ± 3.71**	25.90 ± 4.95
Plasma TG, mM	0.54 ± 0.07	0.50 ± 0.05	0.52 ± 0.09
Plasma Chol, mM	1.76 ± 0.09	1.79 ± 0.09	1.94 ± 0.13

Values are means ± SE; $n = 5$ for chow diet; $n = 7$ for high-metnionine diet (HMD); and $n = 8$ for HMD + 1-trifluoromethoxyphenyl-3-(1-propionylpiperidin-4-*yl*) urea (TPPU). C57BL/6 mice were fed a chow diet or HMD for 8 wk with or without TPPU in drinking water (0.8 $mg \cdot kg^{-1} \cdot day^{-1}$) for 4 wk. Hcy, homocysteine; TG, triglyceride; Chol, cholesterol. $**P < 0.01$ vs. chow diet; $\#P < 0.01$ vs. HMD.

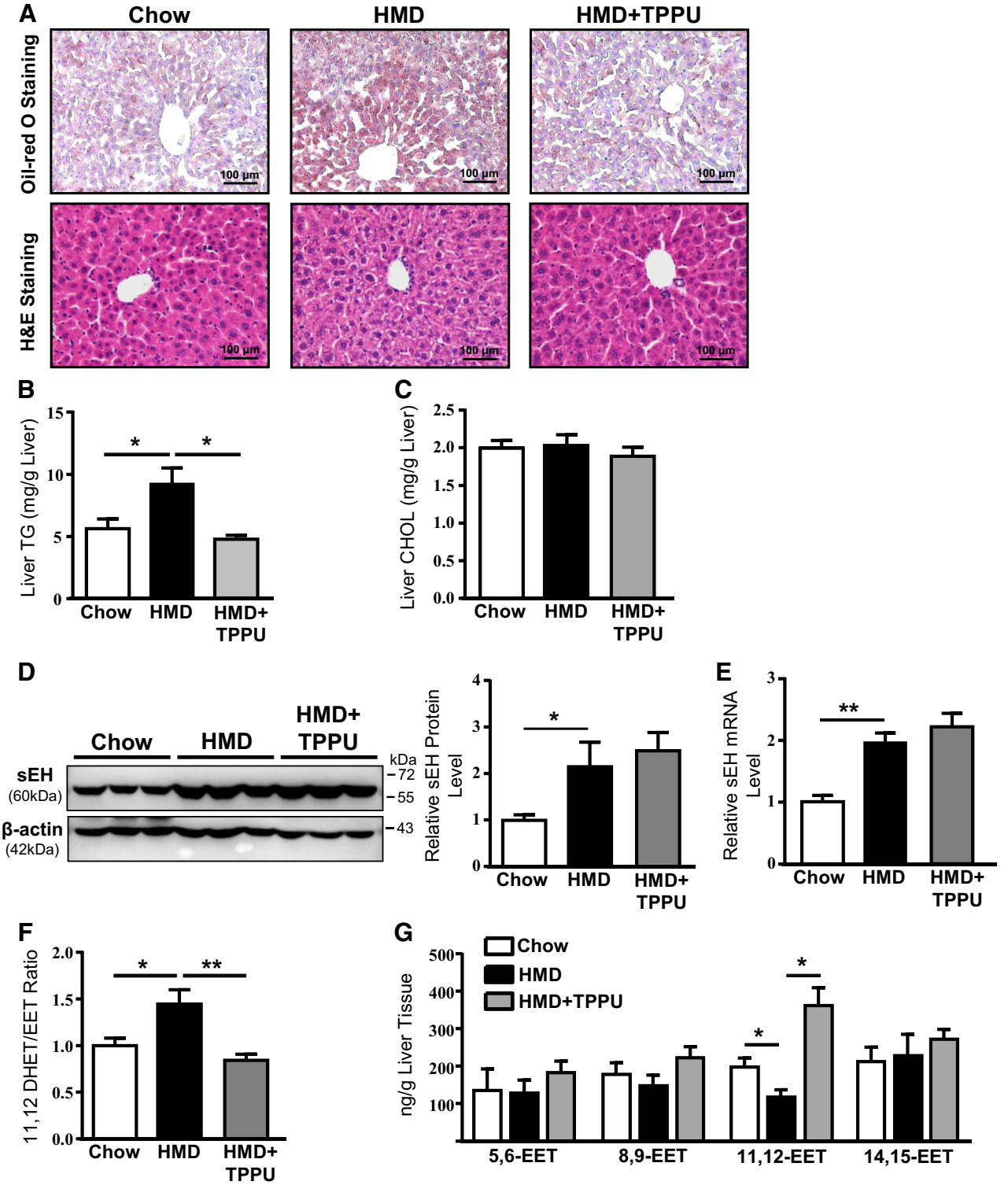

Fig. 3. Inhibition of soluble epoxide hydrolase (sEH) prevented hyperhomocysteinemia (HHcy)-induced hepatic steatosis. Male C57BL/6 mice were fed a chow diet or high-methionine diet (HMD) with or without 1-trifluoromethoxyphenyl-3-(1-propionylpiperidin-4-*yl*) urea (TPPU) in drinking water (0.8 mg·kg^{-1}·day^{-1}) for 4 wk. *A*: representative Oil-red O staining for lipid deposition and hematoxylin and eosin staining for morphological changes in liver. Images were taken at ×200 magnification. *B* and *C*: hepatic triglyceride (TG) and cholesterol (Chol) content. *D*: Western blot analysis (*top*) and quantification (*bottom*) of hepatic sEH protein level in mice with 4-wk treatment. *E*: quantiative PCR analysis of the mRNA level of sEH. *F*: sEH activity was evaluated by the metabolic rate of 11,12-dihydroxyeicosatrienoic acid (DHET) to 11,12-epoxyeicosatrienoic acid (EET) by liquid chromatography with tandem mass spectrometry (LC-MS/MS). *G*: LC-MS/MS analysis of each regioisomer of EETs level in the liver. TG. Data are means ± SE by one-way ANOVA; $n = 5$ for chow diet; $n = 7$ for HMD; and $n = 8$ for HMD + TPPU. *$P < 0.05$, **$P < 0.01$.

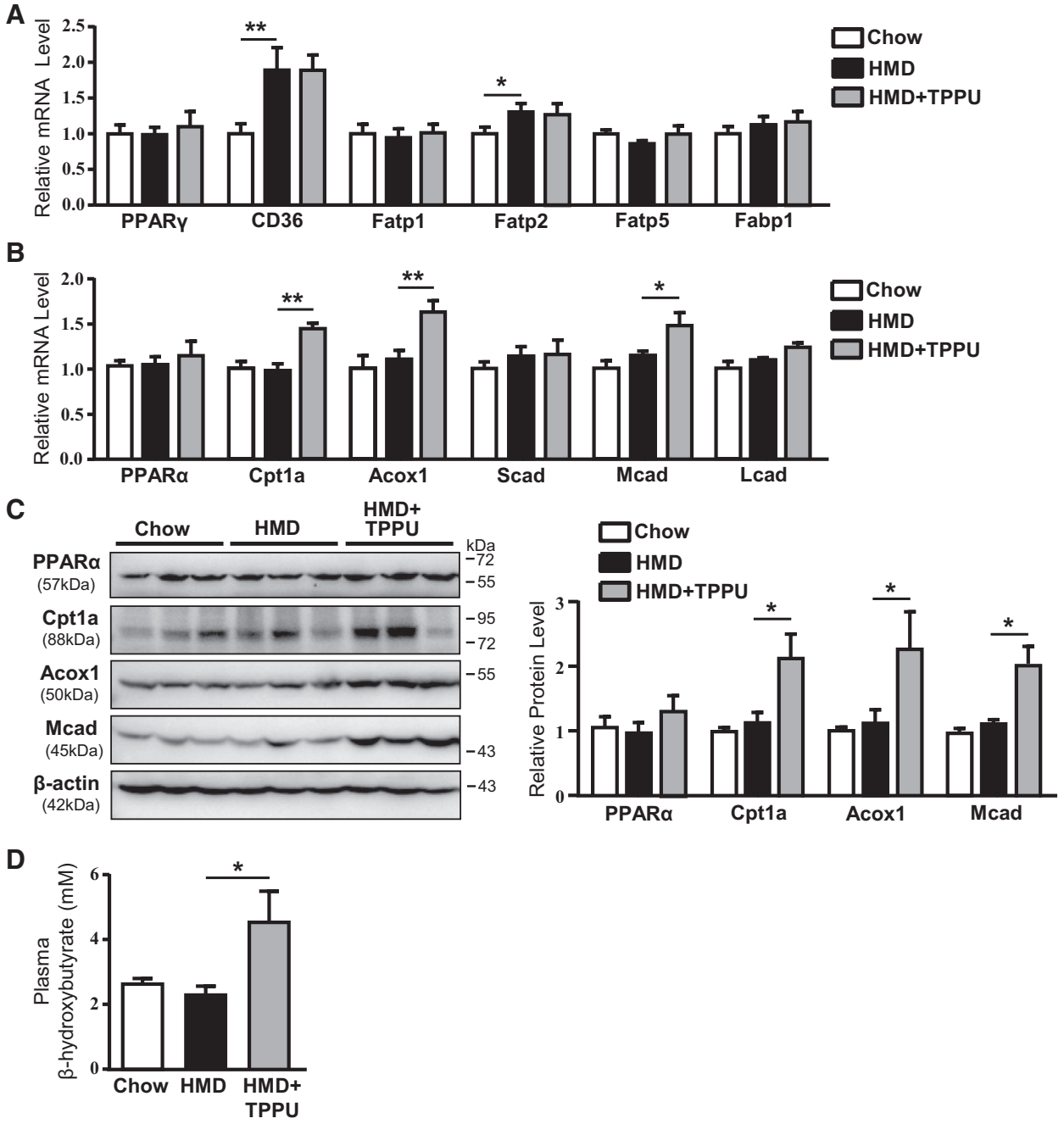

Fig. 4. Inhibition of soluble epoxide hydrolase (sEH) enhanced hepatic fatty acid β-Oxidation. C57BL/6 mice were fed a chow diet or high-methionine diet (HMD) for 8 wk with or without 1-trifluoromethoxyphenyl-3-(1-propionylpiperidin-4-*yl*) urea (TPPU) in drinking water (0.8 mg·kg^{-1}·day^{-1}) for 4 wk. *A* and *C*: quantitative PCR analysis of mRNA levels of genes involved in hepatic fatty acid uptake and fatty acid oxidation. *C*: Western blot analysis (*left*) and quantification (*right*) of peroxisome proliferator-activated receptor-α (PPAR-α) and target genes protein content in the liver. β-Actin was an internal control. *D*: plasma level of β-hydroxybutyrate in mice. Cpt1a, carnitine palmitoyl transferase 1a; Acox1, acyl-coenzyme A oxidase 1; Scad, Mcad, and Lcad, short-, medium- and long-chain acyl-coenzyme A dehydrogenase; Fatp, fatty acid transporter protein; Fabp, fatty acid binding protein. Data are means ± SE by one-way ANOVA. $n = 5$ for chow diet; $n = 7$ for HMD; and $n = 8$ for HMD + TPPU. $^*P < 0.05$, $^{**}P < 0.01$.

mM $CaCl_2$ + 0.05% collagenase I) to flow though the liver for isolating hepatocytes. Hepatocytes were collected from the perfused liver passing through a 400-screen size filter by centrifugation at 50 *g* for 2 min, then resuspended and cultured in RPMI 1640 medium containing 10% fetal bovine serum. After a 6-h attachment, cells were need for the experiments described.

Transient transfection and luciferase activity assay. Murine primary hepatocytes were transfected with PPRE-luciferase reporter plasmid by use of Lipofectamine3000 according to the manufacturer's protocol. The β-galactosidase plasmid was cotransfected as a transfection control. After transfection, cells were lysed in five times reporter buffer and centrifuged at 12,000 *g* for 10 min. The supernatant was collected and used for luciferase activity measurement.

Lipidomic analysis. Hepatic tissue was prepared for lipidomic analysis as described previously (11). Approximately 40 mg liver tissue was homogenized and lysed with 500 μl methanol spiked with

Table 5. *The mRNA levels of genes involved in lipogenesis and triglyceride secretion in chow- and HMD-fed and HMD + soluble epoxide hydrolase inhibitor (TPPU) mice liver*

Lipid Metabolism Genes	Chow	HMD	HMD + TPPU
Lipogenesis			
Lxrα	1 ± 0.04	0.91 ± 0.06	0.96 ± 0.04
Fas	1 ± 0.18	0.84 ± 0.15	0.98 ± 0.14
Acc	1 ± 0.09	0.84 ± 0.11	0.86 ± 0.04
Srebp1	1 ± 0.14	0.77 ± 0.09	0.75 ± 0.12
Chrebp	1 ± 0.10	1.01 ± 0.09	1.10 ± 0.12
Triglyceride secretion			
ApoB	1 ± 0.09	0.88 ± 0.11	1.04 ± 0.16
Mtp	1 ± 0.11	0.95 ± 0.10	1.04 ± 0.13

Values are means ± SE; $n = 5$ for chow diet; $n = 7$ for high-metnionine diet (HMD); and $n = 8$ for HMD + 1-trifluoromethoxyphenyl-3-(1-propionylpiperidin-4-*yl*) urea (TPPU). C57BL/6 mice were fed a chow diet or HMD for 8 wk with or without TPPU in drinking water (0.8 mg·kg^{-1}·day^{-1}) for 4 wk.

IS mixture. After vigorous mixture and centrifugation, the supernatant was collected and transferred to a new tube. Ethyl acetate was added to further extract the sample, and then, the upper organic phase was evaporated. The dried residue was dissolved in 100 μl of 30% acetonitrile. Samples were filtered by using centrifuge tube filters after vigorous mixing before analysis. The ratio of 11,12- dihydroxyeicosatrienoic acid (DHET) to 11,12-EET by liquid chromatography with tandem mass spectrometry (LC-MS/MS) was used to indicate sEH activity.

Histology. Cryosections of liver tissue were excised and fixed in 4% paraformaldehyde for 6 h and dehydrated in 30% sucrose solution overnight and then embedded and stained with 0.3% Oil-red O to visualize lipid droplets. Another portion of the liver was fixed in 10% neutral buffered formalin overnight and then embedded in paraffin wax. Sequential 5-μm paraffin-embedded sections were prepared and stained with hematoxylin and eosin to evaluate morphological changes. Oil-red O staining of hepatocytes was performed with cells fixed in 4% paraformaldehyde for 10 min and stained with 0.3% Oil-red O working solution for 30 min. Images of Oil-red O staining for cells were quantified by using ImageJ.

Quantification of hepatic triglyceride and total cholesterol levels. An amount of 50 mg mouse liver tissue was homogenized at 4°C and extracted in 1 ml chloroform-methanol extraction buffer (2:1). After a 16-h extraction, liver samples were neutralized with 300 μl deionized water and then centrifuged at 12 000 *g* for 10 min. The supernatant was collected, and dried lipid residues were dissolved in 200 μl 5% TritonX-100. Total cholesterol and triglyceride extractions were quantified by using triglyceride or cholesterol determination kits from Thermo Scientific and Wako.

Quantitative PCR assay. Liver tissues and hepatocytes were homogenized, and total RNA was extracted and reverse transcribed to cDNA as templates for qPCR. The levels of target genes were calculated by the $2^{-\Delta Ct}$ method and normalized to that of β-actin in normal control. Sequences of primers used for qPCR are in Table 2.

Western blot analysis. Total protein was extracted and separated by 10% or 5% SDS-PAGE and transferred onto PVDF membranes. The blots were incubated with primary antibodies (sEH, 1:1,000, rabbit polyclonal antibody, no. 10010146; PPAR-α, 1:1,000, rabbit polyclonal antibody, no. 101710; Cpt1a, 1:1,000, rabbit polyclonal antibody, no. 15184-1-AP; Acox1, 1:1,000, rabbit polyclonal antibody, no. 10957-1-AP; Mcad, 1:1,000, rabbit polyclonal antibody, no. 55210-1-AP; and β-actin, 1:4,000, mouse monoclonal antibody; no. 66009-1-Ig). The specificity of antibody against sEH was tested by use of sEH blocking peptide with different ratios of sEH antibody to blocking peptide (no. 10010147; Cayman Chemical). An anti-rabbit or anti-mouse IgG horseradish peroxidase-conjugated secondary antibody was diluted 1:2,000 in 5% milk and incubated for 1 h at room temperature. Densitometric analyses of Western blots were performed using ImageJ software. The expression of selected proteins was normalized to that of the β-actin.

Statistical analysis. Data are presented as means ± SE. Differences between groups were analyzed by unpaired *t*-test or one-way ANOVA with Bonferroni posttest with comparison of more than two groups. Statistical significance was set at $P < 0.05$. Statistical analysis involved use of GraphPad Prism 5.01 (San Diego, CA).

RESULTS

HHcy induced hepatic steatosis and upregulated the expression of sEH in mouse liver. To investigate the role of sEH in HHcy-induced hepatic steatosis, 6-wk-old male C57BL/6 mice were given a chow diet or HMD for 8 wk to establish the HHcy model. Plasma Hcy level was sixfold higher with the HMD than control diet (20.58 ± 2.18 vs. 3.34 ± 0.80, $P < 0.01$) (Table 3). Clinically, three ranges of HHcy are defined: moderate (15–30 μmol/l), intermediate (31–100 μmol/l), and severe (>100 μmol/l). The mean plasma level of Hcy in NAFLD patients was reported to be 15.74 μmol/l (38). Thus our animal model was a mimic of moderate HHcy in humans. High methionine supplementation also resulted in increased liver/body weight ratio, without altering body weight or plasma cholesterol and triglyceride levels (Table 3). As we previously reported, HHcy markedly induced lipid accumulation in the liver (Fig. 1*A*) and increased hepatic triglyceride content (Fig. 1*B*). The hepatic level of cholesterol was not affected (Fig. 1*C*). The specificity of sEH antibody in the liver tissue was verified by use of sEH blocking peptide with different ratios of sEH antibody to blocking peptide (Fig. 1*D*). Importantly, the expression and activity of sEH in the liver was significantly increased by HHcy (Fig. 1, *D* and *E*).

EETs are largely hydrolyzed to their respective inactive diol metabolites by sEH, which suggests that sEH activity is a crucial determinant of EETs bioavailability. We next analyzed the hepatic levels of EETs in mice fed a chow diet or HMD. LC-MS/MS revealed decreased hepatic content of 11,12-EET but not 5,6-; 8,9-; and 14,15-EET with HHcy (Fig. 1*G*). The expression of major genes involved in EET biosynthesis was not altered by HHcy (Fig. 1*H*), which suggests that the decreased 11,12-EET level was caused by increased hydrolysis activity.

Then, we examined the effect of Hcy on lipid metabolism and sEH expression in vitro. Hcy at 100 μM markedly induced intracellular lipid accumulation and sEH expression in primary mouse hepatocytes (Fig. 2, *A–C*). In line with the in vivo study, sEH activity was increased and 11,12-EET level decreased in Hcy-treated hepatocytes (Fig. 2, *D* and *E*).

Inhibition of sEH protected against HHcy-induced hepatic steatosis. To assess the contribution of sEH to disease progression, we fed mice an HMD for 8 wk. Half of the mice were treated with TPPU (0.8 mg·kg^{-1}·day^{-1} by drinking water) for 4 wk starting from the fifth week. TPPU treatment did not affect body weight or plasma cholesterol and triglyceride levels (Table 4) but greatly attenuated HHcy-induced hepatic lipid deposition and triglyceride content (Fig. 3, *A–C*). However, the HHcy-increased activity of sEH and HHcy-decreased level of 11,12-EET reverted toward normal with TPPU treatment (Fig. 3, *F* and *G*). These data suggest that sEH inhibition has a protective effect on HHcy-induced steatosis by increasing the levels of EETs.

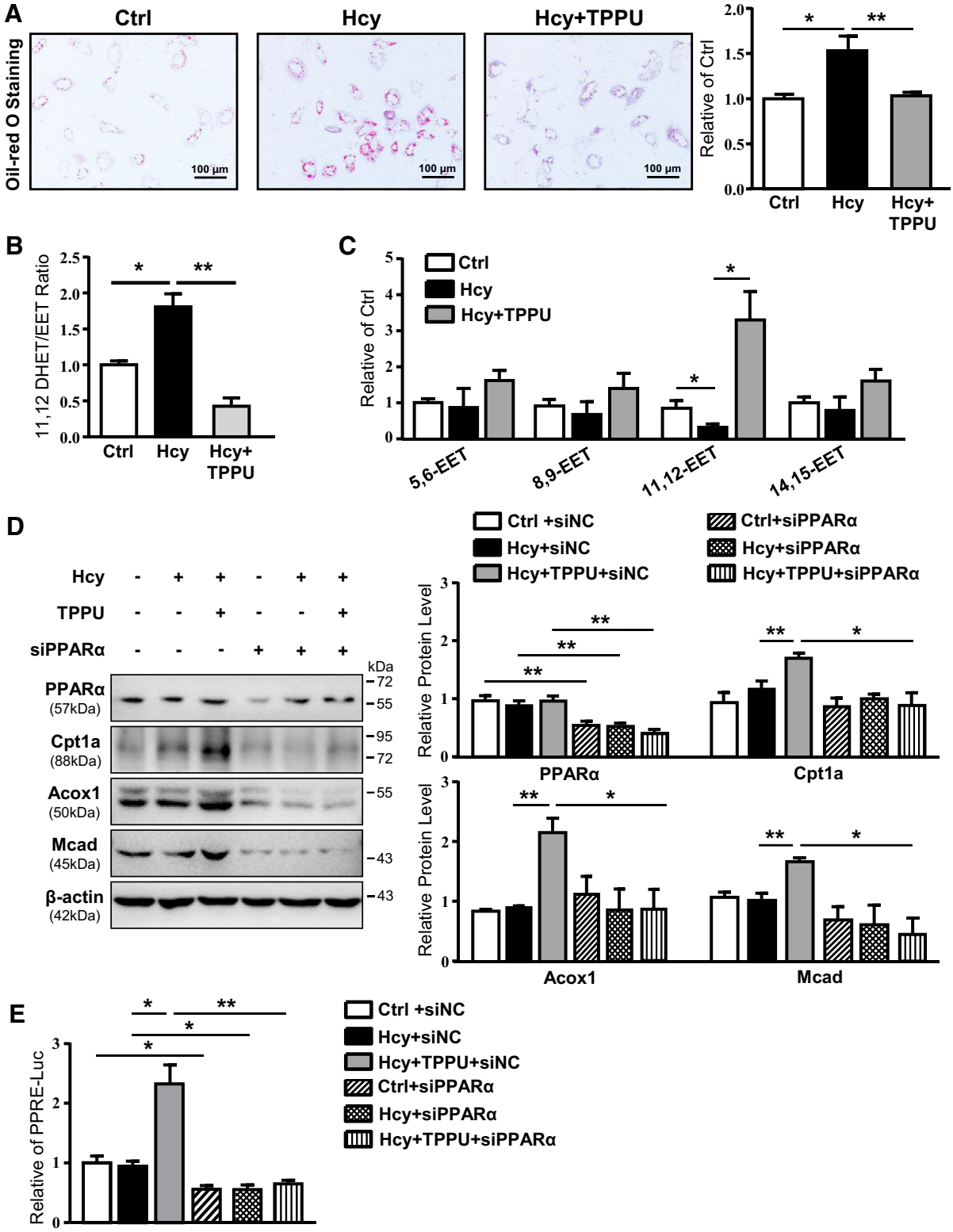

Fig. 5. Inhibition of soluble epoxide hydrolase (sEH) activated peroxisome proliferator-activated receptor-α (PPAR-α) in hepatocytes. *A–C*: murine primary hepatocytes were incubated with Hcy with or without 1-trifluoromethoxyphenyl-3-(1-propionylpiperidin-4-*yl*) urea (TPPU); 1 μM) for 24 h. *A*: Oil-red O staining of representative images (*left*) and quantification (*right*) of intracellular lipid deposition. Images were taken at ×200 magnification. *B*: sEH activity was evaluated by the metabolic rate of 11,12-dihydroxyeicosatrienoic acid (DHET) to 11,12-epoxyeicosatrienoic acid (EET) by liquid chromatography with tandem mass spectrometry (LC-MS/MS). *C*: LC-MS/MS analysis of each regioisomer of EET level in hepatocytes. *D* and *E*: hepatocytes were treated with Hcy with or without TPPU for 24 h after siRNA transfection of PPAR-α (siPPAR-α) or negative control (siNC) for 36 h. *D*: Western blot analysis (*left*) and quantification (*right*) of PPAR-α and protein levels of target genes. β-Actin was an internal control. *E*: relative PPAR-response element (PPRE) luciferase activity. Cpt1a, carnitine palmitoyl transferase 1a; Acox1, acyl-coenzyme A oxidase 1;, Mcad, medium-chain acyl-coenzyme A dehydrogenase. Data are means ± SE of 3 independent experiments by one-way ANOVA. $^{*}P < 0.05$; $^{**}P < 0.01$.

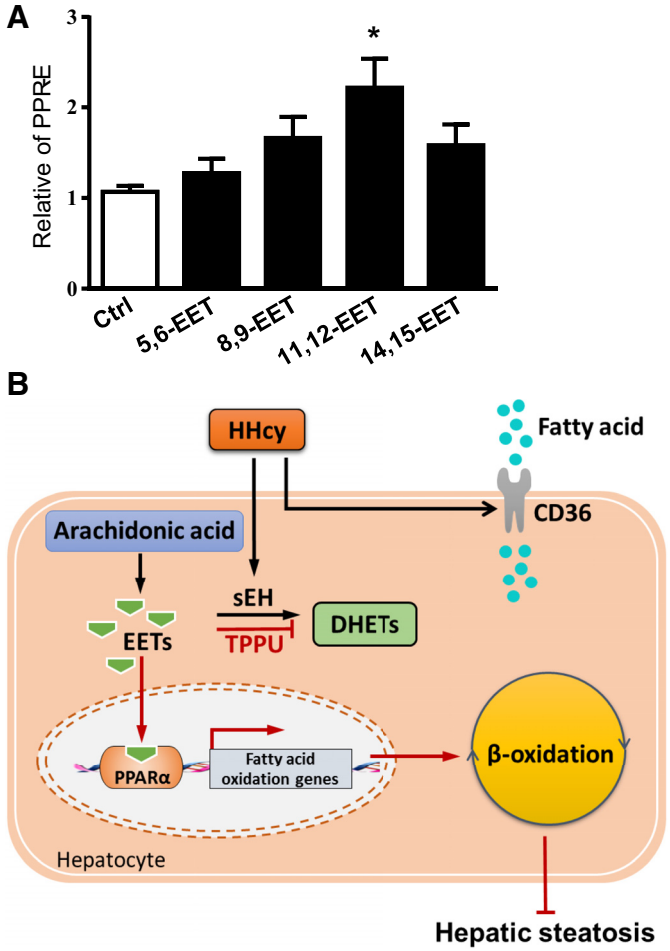

Fig. 6. Activation of peroxisome proliferator-activated receptor-α (PPAR-α) depends on 11,12-epoxyeicosatrienoic acid (EET). *A*: primary hepatocytes were transfected with PPAR-response element (PPRE)-luciferase reporter for 36 h, then treated with each regioisomer of EETs (100 nM) for 24 h. Data are means ± SE of 3 independent experiments by unpaired *t*-test. $*P < 0.05$ vs. Ctrl. *B*: proposed mechanism of improvement of hyperhomocysteinemia (HHcy)-induced hepatic steatosis by sEH inhibitor in liver. High levels of Hcy induced fatty acid uptake by upregulating of CD36. Inhibition of soluble epoxide hydrolase (sEH) prevented EETs degradation from HHcy. As an endogenous activator of PPAR-α, EETs promotes the binding of PPAR-α to target genes, which facilitates the β-oxidation of fatty acids and lipid removal from the liver. DHET, 11,12-dihydroxyeicosatrienoic acid; TPPU, 1-trifluoromethoxyphenyl-3-(1-propionylpiperidin-4-*yl*) urea.

Inhibition of sEH enhanced β-oxidation of hepatic fatty acids. To understand how sEH inhibition alleviates HHcy-induced lipid disorder, we analyzed the expression of genes involved in lipid metabolism, including lipogenesis, triglyceride secretion, fatty acid uptake and oxidation, in mouse liver. Administration of the sEH inhibitor did not inhibit the HHcy-upregulated CD36 and fatty acid transporter membrane 2, but effectively activated PPAR-α, as evidenced by elevated mRNA levels of Cpt1a, Acox1, and Mcad (Fig. 4, *A* and *B*). In parallel, the protein levels of Cpt1a, Acox1, and Mcad were increased by sEH inhibition (Fig. 4*C*). The expression of other related genes remained unchanged (Table 5). Notably, TPPU treatment augmented plasma β-hydroxybutyrate level, an indicator of increased hepatic fatty acid β-oxidation in plasma, as compared with HHcy mouse plasma (Fig. 4*D*). Moreover, under the normal condition, TPPU had no effect on lipid deposition and hepatic content of cholesterol and triglycerides with a significant reduction in sEH activity (data not shown). Together, these data indicate that activation of PPAR-α by TPPU facilitates hepatic fatty acid β-oxidation and alleviates HHcy-induced hepatic steatosis.

Inhibition of sEH activated PPAR-α in the liver and promoted the β-oxidation of fatty acid. We next studied the mechanism of sEH inhibition increasing the β-oxidation of fatty acids by treating hepatocytes with Hcy or Hcy + TPPU. Inhibition of sEH abolished Hcy-increased lipid accumulation, sEH activity, and 11,12-EET level (Fig. 5, *A–C*). Consistent with in vivo results, the expression of genes involved in the β-oxidation of fatty acids was reinforced in cultured hepatocytes with TPPU treatment, which was reversed by knockdown of PPAR-α (Fig. 5*D*). To further determine the direct effect of TPPU on PPAR-α activation, we transfected a PPRE-luciferase reporter plasmid in cultured hepatocytes with or without Hcy stimulation. TPPU greatly increased PPRE-luciferase activity in Hcy-treated hepatocytes, which was inhibited by PPAR-α knockdown (Fig. 5*E*) and suggests a key role for PPAR-α in TPPU-induced β-oxidation of fatty acids in the liver of HHcy mice.

Transcriptional activity of PPAR-α depends on 11,12-EET. The PPAR-s have three isoforms, PPAR-α, PPAR-β/δ, and PPAR-γ, which are expressed differentially in tissues with various biological functions. Several studies provided a link between arachidonic acid metabolism and PPAR activation, with a focus on the proposed endogenous ligands produced by the cytochrome -*P*450 oxidase pathway (54). PPAR-α has a major role in the β-oxidation of the fatty acid pathway in the liver-metabolizing lipids and lipoproteins (6). Of note, 11,12-EET is a novel endogenous activator of PPAR-α in primary rat hepatocytes (35). To definite which isoform of EETs was essential for the activation of PPAR-α, we incubated hepatocytes with the four isoforms of EETs (100 nM) to mimic the function of endogenous EETs. 11,12-EET but not the other three EETs significantly increased the luciferase activity in hepatocytes transfected with PPRE (Fig. 6*A*). Hence, 11,12-EET ligand dependently activates PPAR-α and plays an important role in the use of excess lipid induced by HHcy in the liver.

DISCUSSION

sEH enzymatically catalyzes the conversion of EETs and other EpFAs to the corresponding inactive or less active diols, which are responsible for decreasing the levels of EETs and EpFAs, thus diminishing their benefit for cardiovascular disease (18, 22). However, the role of sEH in modulating lipid metabolism in the liver is unknown. Recently, inhibition of sEH was found to attenuate high-fat diet-induced hepatic steatosis (31), thus demonstrating that sEH is a potential therapeutic target for lipid disturbance in the liver. HHcy is a risk factor for fatty liver disease. Our previous study showed that sEH participated in Hcy-induced endothelial dysfunction (59).

In this study, we defined the role of sEH in Hcy-induced hepatic steatosis and explored the underlying mechanism. Our novel findings include that *1*) HHcy upregulates sEH expression and activity in vivo and in vitro; *2*) inhibition of sEH alleviates HHcy-induced hepatic lipid accumulation by elevat-

ing fatty acid β-oxidation; and *3*) 11,12-EET is involved as endogenous ligands for PPAR-α activation, which plays a vital role in ameliorating HHcy-induced hepatic steatosis.

In the liver, the imbalance in lipid availability and disposal leads to hepatic lipid accumulation. We previously reported that HHcy enhanced CD36 expression and contributed to lipid accumulation in the liver (56). However, simultaneous application of TPPU and HHcy had no effect on the upregulation of CD36 by HHcy but significantly increased fatty acid β-oxidation gene expression. Notably, silencing PPAR-α expression significantly reduced the expression of those genes caused by simultaneous administration of TPPU and HHcy in hepatocytes, which suggests that sEH inhibition increases lipid oxidation in the liver. Our data support that PPAR-α plays an essential role in maintaining lipid metabolism in the HHcy mouse model.

The pharmacological potency of sEH inhibition is a combined function of the drug potency and the effective amount of the drug at the target site. In the past few years, numerous sEH inhibitors have been synthesized and applied to inhibit enzyme activity of sEH (24, 25, 30, 32). Some early sEH inhibitors were designed to mimic EETs with the amide or urea central pharmacophore being isosteric with the epoxide and thus act both as EpFA mimics and sEH inhibitors. One such compound is 12-(3-adamantan-1-*yl*-ureido)dodecanoic acid (13). 12-(3-Adamantan-1-*yl*-ureido) was later shown to have EET-like effects in the absence of the sEH in a tissue (37). Later compounds such as the selective sEH inhibitor TPPU we used do not have structures anticipated to bind directly to a putative EET receptor and are highly selective sEH inhibitors of both mouse and human sEH (29, 44). TPPU, a second-generation sEH inhibitor from the Bruce Hommack laboratory, is one of the most promising drug compounds for sEH inhibition. The potency of TPPU to inhibit sEH is high (human IC_{50}: 0.9 nM; rat IC_{50}: 5 nM and mice IC_{50}: 6 nM) and it has been used in several animal disease models (41, 42, 46). Studies of the pharmacokinetic parameters of 11 sEH inhibitors in cynomolgus monkeys showed that TPPU had higher potency (IC_{50} in the low nM range), physicochemical properties consistent with drug likeness, pharmacokinetic properties with relatively rapid absorption, high area under the curve, and long half-life that would facilitate long-term interventional studies (49).

Inhibition of sEH is potentially beneficial because it increases and prolongs the functional effect of EETs and other EpFAs (14). As metabolites of arachidonic acid by sEH, EETs have important anti-inflammatory effects and cardiovascular protective effects. However, the role of EETs regioisomers is different in different disease models. The serum level of 14,15-EET was decreased in the aging-related insulin-resistance mouse model (55). 5,6- and 8,9-EET induced de novo vascularization and promoted the formation of functionally intact vessels as angiogenic lipids in a subcutaneous sponge model (39). Moreover, 11,12-EET had higher anti-inflammatory and vascular protective effects as compared with 14,15-EET (36). In our study, we found that HHcy decreased the level of 11,12-EET rather than the other three isoforms, so the protective effect of the sEH inhibitor in HHcy-induced hepatic steatosis was specifically mediated by 11,12-EET. Our results were consistent with previous findings that 11,12-EET preferentially activated PPAR-α in rat hepatocytes (35). Therefore, we propose PPAR-α as a potential target for 11,12-EET in the liver.

A causal finding of the current study is that in the HHcy-induced liver injury model, HHcy treatment did not inhibit the activation of PPAR-α although it reduced hepatic 11,12-EET level. One reason for this finding is that fatty acids are also known to activate PPAR-α in the liver, which may be caused by a compensatory effect of lipid overload (47). For instance, abdominally obese male humans had significantly higher fatty acid β-oxidation of dietary fat than did lean males (19). In the obese rat model, liver mitochondria exhibit higher fatty acid β-oxidation capacity (27). However, further enhanced fatty acid β-oxidation was found an effective therapeutic strategy to alleviate hepatic steatosis (1, 21, 47). Nevertheless, sEH inhibition significantly activated PPAR-α and favored hepatic fatty acid β-oxidation, thereby improving hepatic lipid deposition. Our study reveals that sEH inhibition is beneficial for HHcy-induced hepatic steatosis.

In summary, we have demonstrated that in the liver, sEH plays a prominent role in HHcy-induced lipid disorder. Improving hepatic steatosis in HHcy mice by pharmacological inhibition of sEH to activate PPAR-α was ligand dependent, and sEH could be a promising target for treating HHcy-induced hepatic steatosis.

GRANTS

This work was supported in part by Ministry of Science and Technology of China Grant 2016YFC0903000; National Natural Science Foundation of China Grants 81420108003, 81790621, 81700506, 81770836, and 91539108; Tianjin Municipal Science and Technology Project Grant 14JCYBJC41800; and National Institute of Environmental Health Sciences Grant R01-EX-002710.

DISCLOSURES

No conflicts of interest, financial or otherwise, are declared by the authors.

AUTHOR CONTRIBUTIONS

L.Y. and Y.Z. conceived and designed research; L.Y., B.-Y.C., Q.C., and W.-B.C, performed experiments; L.Y., C.-J.Y., J.L., and W.-L.L analyzed data; L.Y., and L.T. interpreted results of experiments; L.Y., M.Y., B.-C.L and J.-L.H prepared figures; L.Y., S.H.H, X.Z., C.-J.W., and Y.Z. drafted manuscript; L.Y., D.A., B.D.H, and Y.Z. edited and revised manuscript; L.Y., B.-Y.C., Q.C., W.-B.C, C.-J.Y., J.L., W.-L.L, L.T., M.Y., B.-C.L, J.-L.H, S.H.H, X.Z., C.-J.W., D.A., B.D.H, and Y.Z. approved final version of manuscript.

REFERENCES

1. **Abdelmegeed MA, Yoo SH, Henderson LE, Gonzalez FJ, Woodcroft KJ, Song BJ.** PPARalpha expression protects male mice from high fat-induced nonalcoholic fatty liver. *J Nutr* 141: 603–610, 2011. doi:10.3945/jn.110.135210.
2. **Angulo P.** Nonalcoholic fatty liver disease. *N Engl J Med* 346: 1221–1231, 2002. doi:10.1056/NEJMra011775.
3. **Audelin MC, Genest J Jr.** Homocysteine and cardiovascular disease in diabetes mellitus. *Atherosclerosis* 159: 497–511, 2001. doi:10.1016/S0021-9150(01)00531-7.
4. **Barbier O, Torra IP, Duguay Y, Blanquart C, Fruchart JC, Glineur C, Staels B.** Pleiotropic actions of peroxisome proliferator-activated receptors in lipid metabolism and atherosclerosis. *Arterioscler Thromb Vasc Biol* 22: 717–726, 2002. doi:10.1161/01.ATV.0000015598.86369.04.
5. **Bocher V, Pineda-Torra I, Fruchart JC, Staels B.** PPARs: transcription factors controlling lipid and lipoprotein metabolism. *Ann N Y Acad Sci* 967: 7–18, 2002. doi:10.1111/j.1749-6632.2002.tb04258.x.
6. **Burri L, Thoresen GH, Berge RK.** The role of PPARα activation in liver and muscle. *PPAR Res* 2010: 542359, 2010. doi:10.1155/2010/542359.
7. **Chen G, Xu R, Zhang S, Wang Y, Wang P, Edin ML, Zeldin DC, Wang DW.** CYP2J2 overexpression attenuates nonalcoholic fatty liver

disease induced by high-fat diet in mice. *Am J Physiol Endocrinol Metab* 308: E97–E110, 2015. doi:10.1152/ajpendo.00366.2014.

8. **Clarke R, Daly L, Robinson K, Naughten E, Cahalane S, Fowler B, Graham I.** Hyperhomocysteinemia: an independent risk factor for vascular disease. *N Engl J Med* 324: 1149–1155, 1991. doi:10.1056/NEJM199104253241701.
9. **Dai H, Wang W, Tang X, Chen R, Chen Z, Lu Y, Yuan H.** Association between homocysteine and non-alcoholic fatty liver disease in Chinese adults: a cross-sectional study. *Nutr J* 15: 102, 2016. doi:10.1186/s12937-016-0221-6.
10. **Dai Y, Zhu J, Meng D, Yu C, Li Y.** Association of homocysteine level with biopsy-proven non-alcoholic fatty liver disease: a meta-analysis. *J Clin Biochem Nutr* 58: 76–83, 2016. doi:10.3164/jcbn.15-54.
11. **Ding Y, Li Y, Zhang X, He J, Lu D, Fang X, Wang Y, Wang J, Zhang Y, Qiao X, Gan LM, Chen C, Zhu Y.** Soluble epoxide hydrolase activation by S-nitrosation contributes to cardiac ischemia-reperfusion injury. *J Mol Cell Cardiol* 110: 70–79, 2017. doi:10.1016/j.yjmcc.2017.07.006.
12. **Fan JG.** Epidemiology of alcoholic and nonalcoholic fatty liver disease in China. *J Gastroenterol Hepatol* 28, *Suppl* 1: 11–17, 2013. doi:10.1111/jgh.12036.
13. **Fang X, Hu S, Watanabe T, Weintraub NL, Snyder GD, Yao J, Liu Y, Shyy JY, Hammock BD, Spector AA.** Activation of peroxisome proliferator-activated receptor alpha by substituted urea-derived soluble epoxide hydrolase inhibitors. *J Pharmacol Exp Ther* 314: 260–270, 2005. doi:10.1124/jpet.105.085605.
14. **Fang X, Kaduce TL, Weintraub NL, Harmon S, Teesch LM, Morisseau C, Thompson DA, Hammock BD, Spector AA.** Pathways of epoxyeicosatrienoic acid metabolism in endothelial cells. Implications for the vascular effects of soluble epoxide hydrolase inhibition. *J Biol Chem* 276: 14867–14874, 2001. doi:10.1074/jbc.M011761200.
15. **Gulsen M, Yesilova Z, Bagci S, Uygun A, Ozcan A, Ercin CN, Erdil A, Sanisoglu SY, Cakir E, Ates Y, Erbil MK, Karaeren N, Dagalp K.** Elevated plasma homocysteine concentrations as a predictor of steatohepatitis in patients with non-alcoholic fatty liver disease. *J Gastroenterol Hepatol* 20: 1448–1455, 2005. doi:10.1111/j.1440-1746.2005.03891.x.
16. **Hao L, Ma J, Zhu J, Stampfer MJ, Tian Y, Willett WC, Li Z.** High prevalence of hyperhomocysteinemia in Chinese adults is associated with low folate, vitamin B-12, and vitamin B-6 status. *J Nutr* 137: 407–413, 2007. doi:10.1093/jn/137.2.407.
17. **Hashimoto T, Cook WS, Qi C, Yeldandi AV, Reddy JK, Rao MS.** Defect in peroxisome proliferator-activated receptor alpha-inducible fatty acid oxidation determines the severity of hepatic steatosis in response to fasting. *J Biol Chem* 275: 28918–28928, 2000. doi:10.1074/jbc.M910350199.
18. **He J, Wang C, Zhu Y, Ai D.** Soluble epoxide hydrolase: A potential target for metabolic diseases. *J Diabetes* 8: 305–313, 2016. doi:10.1111/1753-0407.12358.
19. **Hodson L, McQuaid SE, Humphreys SM, Milne R, Fielding BA, Frayn KN, Karpe F.** Greater dietary fat oxidation in obese compared with lean men: an adaptive mechanism to prevent liver fat accumulation? *Am J Physiol Endocrinol Metab* 299: E584–E592, 2010. doi:10.1152/ajpendo.00272.2010.
21. **Huang J, Jia Y, Fu T, Viswakarma N, Bai L, Rao MS, Zhu Y, Borensztajn J, Reddy JK.** Sustained activation of PPARα by endogenous ligands increases hepatic fatty acid oxidation and prevents obesity in ob/ob mice. *FASEB J* 26: 628–638, 2012. doi:10.1096/fj.11-194019.
22. **Imig JD, Hammock BD.** Soluble epoxide hydrolase as a therapeutic target for cardiovascular diseases. *Nat Rev Drug Discov* 8: 794–805, 2009. doi:10.1038/nrd2875.
23. **Ji C, Kaplowitz N.** Hyperhomocysteinemia, endoplasmic reticulum stress, and alcoholic liver injury. *World J Gastroenterol* 10: 1699–1708, 2004. doi:10.3748/wjg.v10.i12.1699.
24. **Kim IH, Morisseau C, Watanabe T, Hammock BD.** Design, synthesis, and biological activity of 1,3-disubstituted ureas as potent inhibitors of the soluble epoxide hydrolase of increased water solubility. *J Med Chem* 47: 2110–2122, 2004. doi:10.1021/jm030514j.
25. **Kim IH, Tsai HJ, Nishi K, Kasagami T, Morisseau C, Hammock BD.** 1,3-disubstituted ureas functionalized with ether groups are potent inhibitors of the soluble epoxide hydrolase with improved pharmacokinetic properties. *J Med Chem* 50: 5217–5226, 2007. doi:10.1021/jm070705c.
27. **Lazarin MO, Ishii-Iwamoto EL, Yamamoto NS, Constantin RP, Garcia RF, da Costa CE, Vitoriano AS, de Oliveira MC, Salgueiro-Pagadigorria CL.** Liver mitochondrial function and redox status in an experimental model of non-alcoholic fatty liver disease induced by monosodium L-glutamate in rats. *Exp Mol Pathol* 91: 687–694, 2011. doi:10.1016/j.yexmp.2011.07.003.
28. **Li Z, Xue J, Chen P, Chen L, Yan S, Liu L.** Prevalence of nonalcoholic fatty liver disease in mainland of China: a meta-analysis of published studies. *J Gastroenterol Hepatol* 29: 42–51, 2014. doi:10.1111/jgh.12428.
29. **Liu JY, Lin YP, Qiu H, Morisseau C, Rose TE, Hwang SH, Chiamvimonvat N, Hammock BD.** Substituted phenyl groups improve the pharmacokinetic profile and anti-inflammatory effect of urea-based soluble epoxide hydrolase inhibitors in murine models. *Eur J Pharm Sci* 48: 619–627, 2013. doi:10.1016/j.ejps.2012.12.013.
30. **Liu JY, Tsai HJ, Hwang SH, Jones PD, Morisseau C, Hammock BD.** Pharmacokinetic optimization of four soluble epoxide hydrolase inhibitors for use in a murine model of inflammation. *Br J Pharmacol* 156: 284–296, 2009. doi:10.1111/j.1476-5381.2008.00009.x.
31. **Liu Y, Dang H, Li D, Pang W, Hammock BD, Zhu Y.** Inhibition of soluble epoxide hydrolase attenuates high-fat-diet-induced hepatic steatosis by reduced systemic inflammatory status in mice. *PLoS One* 7: e39165, 2012. doi:10.1371/journal.pone.0039165.
32. **Morisseau C, Goodrow MH, Dowdy D, Zheng J, Greene JF, Sanborn JR, Hammock BD.** Potent urea and carbamate inhibitors of soluble epoxide hydrolases. *Proc Natl Acad Sci USA* 96: 8849–8854, 1999. doi:10.1073/pnas.96.16.8849.
33. **Morisseau C, Hammock BD.** Impact of soluble epoxide hydrolase and epoxyeicosanoids on human health. *Annu Rev Pharmacol Toxicol* 53: 37–58, 2013. doi:10.1146/annurev-pharmtox-011112-140244.
35. **Ng VY, Huang Y, Reddy LM, Falck JR, Lin ET, Kroetz DL.** Cytochrome P450 eicosanoids are activators of peroxisome proliferator-activated receptor alpha. *Drug Metab Dispos* 35: 1126–1134, 2007. doi:10.1124/dmd.106.013839.
36. **Node K, Huo Y, Ruan X, Yang B, Spiecker M, Ley K, Zeldin DC, Liao JK.** Anti-inflammatory properties of cytochrome P450 epoxygenase-derived eicosanoids. *Science* 285: 1276–1279, 1999. doi:10.1126/science.285.5431.1276.
37. **Olearczyk JJ, Field MB, Kim IH, Morisseau C, Hammock BD, Imig JD.** Substituted adamantyl-urea inhibitors of the soluble epoxide hydrolase dilate mesenteric resistance vessels. *J Pharmacol Exp Ther* 318: 1307–1314, 2006. doi:10.1124/jpet.106.103556.
38. **Pastore A, Alisi A, di Giovamberardino G, Crudele A, Ceccarelli S, Panera N, Dionisi-Vici C, Nobili V.** Plasma levels of homocysteine and cysteine increased in pediatric NAFLD and strongly correlated with severity of liver damage. *Int J Mol Sci* 15: 21202–21214, 2014. doi:10.3390/ijms151121202.
39. **Pozzi A, Macias-Perez I, Abair T, Wei S, Su Y, Zent R, Falck JR, Capdevila JH.** Characterization of 5,6- and 8,9-epoxyeicosatrienoic acids (5,6- and 8,9-EET) as potent in vivo angiogenic lipids. *J Biol Chem* 280: 27138–27146, 2005. doi:10.1074/jbc.M501730200.
40. **Reddy JK, Rao MS.** Lipid metabolism and liver inflammation. II. Fatty liver disease and fatty acid oxidation. *Am J Physiol Gastrointest Liver Physiol* 290: G852–G858, 2006. doi:10.1152/ajpgi.00521.2005.
41. **Ren Q, Ma M, Ishima T, Morisseau C, Yang J, Wagner KM, Zhang JC, Yang C, Yao W, Dong C, Han M, Hammock BD, Hashimoto K.** Gene deficiency and pharmacological inhibition of soluble epoxide hydrolase confers resilience to repeated social defeat stress. *Proc Natl Acad Sci USA* 113: E1944–E1952, 2016. doi:10.1073/pnas.1601532113.
42. **Ren Q, Ma M, Yang J, Nonaka R, Yamaguchi A, Ishikawa KI, Kobayashi K, Murayama S, Hwang SH, Saiki S, Akamatsu W, Hattori N, Hammock BD, Hashimoto K.** Soluble epoxide hydrolase plays a key role in the pathogenesis of Parkinson's disease. *Proc Natl Acad Sci USA* 115: E5815–E5823, 2018. doi:10.1073/pnas.1802179115.
43. **Robert K, Nehmé J, Bourdon E, Pivert G, Friguet B, Delcayre C, Delabar JM, Janel N.** Cystathionine beta synthase deficiency promotes oxidative stress, fibrosis, and steatosis in mice liver. *Gastroenterology* 128: 1405–1415, 2005. doi:10.1053/j.gastro.2005.02.034.
44. **Rose TE, Morisseau C, Liu JY, Inceoglu B, Jones PD, Sanborn JR, Hammock BD.** 1-Aryl-3-(1-acylpiperidin-4-yl)urea inhibitors of human and murine soluble epoxide hydrolase: structure-activity relationships, pharmacokinetics, and reduction of inflammatory pain. *J Med Chem* 53: 7067–7075, 2010. doi:10.1021/jm100691c.
45. **Schroecksnadel K, Frick B, Wirleitner B, Winkler C, Schennach H, Fuchs D.** Moderate hyperhomocysteinemia and immune activation. *Curr Pharm Biotechnol* 5: 107–118, 2004. doi:10.2174/1389201043489657.
46. **Sirish P, Li N, Liu JY, Lee KS, Hwang SH, Qiu H, Zhao C, Ma SM, López JE, Hammock BD, Chiamvimonvat N.** Unique mechanistic insights into the beneficial effects of soluble epoxide hydrolase inhibitors

in the prevention of cardiac fibrosis. *Proc Natl Acad Sci USA* 110: 5618–5623, 2013. doi:10.1073/pnas.1221972110.

47. **Tanaka N, Aoyama T, Kimura S, Gonzalez FJ.** Targeting nuclear receptors for the treatment of fatty liver disease. *Pharmacol Ther* 179: 142–157, 2017. doi:10.1016/j.pharmthera.2017.05.011.
49. **Ulu A, Appt S, Morisseau C, Hwang SH, Jones PD, Rose TE, Dong H, Lango J, Yang J, Tsai HJ, Miyabe C, Fortenbach C, Adams MR, Hammock BD.** Pharmacokinetics and in vivo potency of soluble epoxide hydrolase inhibitors in cynomolgus monkeys. *Br J Pharmacol* 165: 1401–1412, 2012. doi:10.1111/j.1476-5381.2011.01641.x.
50. **Verhoef P, van Vliet T, Olthof MR, Katan MB.** A high-protein diet increases postprandial but not fasting plasma total homocysteine concentrations: a dietary controlled, crossover trial in healthy volunteers. *Am J Clin Nutr* 82: 553–558, 2005. doi:10.1093/ajcn/82.3.553.
51. **Wang C, Liu W, Yao L, Zhang X, Zhang X, Ye C, Jiang H, He J, Zhu Y, Ai D.** Hydroxyeicosapentaenoic acids and epoxyeicosatetraenoic acids attenuate early occurrence of nonalcoholic fatty liver disease. *Br J Pharmacol* 174: 2358–2372, 2017. doi:10.1111/bph.13844.
52. **Werstuck GH, Lentz SR, Dayal S, Hossain GS, Sood SK, Shi YY, Zhou J, Maeda N, Krisans SK, Malinow MR, Austin RC.** Homocysteine-induced endoplasmic reticulum stress causes dysregulation of the cholesterol and triglyceride biosynthetic pathways. *J Clin Invest* 107: 1263–1273, 2001. doi:10.1172/JCI11596.
53. **Wong VW, Chu WC, Wong GL, Chan RS, Chim AM, Ong A, Yeung DK, Yiu KK, Chu SH, Woo J, Chan FK, Chan HL.** Prevalence of non-alcoholic fatty liver disease and advanced fibrosis in Hong Kong Chinese: a population study using proton-magnetic resonance spectroscopy and transient elastography. *Gut* 61: 409–415, 2012. doi:10.1136/gutjnl-2011-300342.
54. **Wray J, Bishop-Bailey D.** Epoxygenases and peroxisome proliferator-activated receptors in mammalian vascular biology. *Exp Physiol* 93: 148–154, 2008. doi:10.1113/expphysiol.2007.038612.
55. **Yang Y, Dong R, Chen Z, Hu D, Fu M, Tang Y, Wang DW, Xu X, Tu L.** Endothelium-specific CYP2J2 overexpression attenuates age-related insulin resistance. *Aging Cell* 17: e12718, 2018. doi:10.1111/acel.12718.
56. **Yao L, Wang C, Zhang X, Peng L, Liu W, Zhang X, Liu Y, He J, Jiang C, Ai D, Zhu Y.** Hyperhomocysteinemia activates the aryl hydrocarbon receptor/CD36 pathway to promote hepatic steatosis in mice. *Hepatology* 64: 92–105, 2016. doi:10.1002/hep.28518.
57. **Younossi ZM, Koenig AB, Abdelatif D, Fazel Y, Henry L, Wymer M.** Global epidemiology of nonalcoholic fatty liver disease-Meta-analytic assessment of prevalence, incidence, and outcomes. *Hepatology* 64: 73–84, 2016. doi:10.1002/hep.28431.
58. **Zha W, Edin ML, Vendrov KC, Schuck RN, Lih FB, Jat JL, Bradbury JA, DeGraff LM, Hua K, Tomer KB, Falck JR, Zeldin DC, Lee CR.** Functional characterization of cytochrome P450-derived epoxyeicosatrienoic acids in adipogenesis and obesity. *J Lipid Res* 55: 2124–2136, 2014. doi:10.1194/jlr.M053199.
59. **Zhang D, Xie X, Chen Y, Hammock BD, Kong W, Zhu Y.** Homocysteine upregulates soluble epoxide hydrolase in vascular endothelium in vitro and in vivo. *Circ Res* 110: 808–817, 2012. doi:10.1161/CIRCRESAHA.111.259325.